Tanzania Journal of Science
Volume 51(3), 2025
journal homepage: https://commons.udsm.ac.tz/tjs/

Mathematical analysis of toxicants and diseases impact on a prey-predator system with control interventions

Nuru Yazidi Juma[1,2]*, Thadei Damas Sagamiko[2], and James Philbert Mpele[2]

[1]*Secondary Education Department, Rungwe District, P. O. Box 148 Mbeya, Tanzania*
[2]*Department of Physics, Mathematics and Informatics,*
Dar es Salaam University College of Education, P. O. Box 2329 Dar es Salaam, Tanzania
Co-authors'e-mails: tsagamiko@gmail.com,mweyujames@gmail.com

Keywords

Prey-Predator, Toxicants; Host-specific diseases; Spatial isolation; Bioremedial-Antitoxic.

Abstract

This study developed a generic prey-predator mathematical model incorporating logistic growth for prey and a Holling Type I functional response for predator consumption. Prey-predator interactions form the foundation of ecological balance, but in recent decades these systems have been increasingly threatened by toxicants and infectious diseases. The combined effect of these challenges can lead to severe population declines, biodiversity loss, and ecosystem instability, making their study important for conservation and environmental management. The model includes the effects of diseases and toxicants on prey and toxicants only on predators, and explores optimal control strategies to mitigate these threats. Without considering time delays, the model's stability was examined using differential equation theory. Local stability of equilibrium points was analyzed through Jacobian matrix and eigenvalue methods, while Lyapunov functions were used for analysing global stability. The model was confirmed to be well-posed, meaning its solutions are biologically feasible. Initial simulations without control measures revealed that both diseases and toxicants significantly reduce prey and predator populations. When time-dependent controls were introduced, two strategies were tested: spatial isolation for disease control and bioremedial-antitoxic measures for toxicant control. Results showed that each control strategy independently improved population sizes. However, the best outcomes occurred when both strategies were applied together, leading to the greatest increase in prey and predator populations. The findings highlight that integrated control measures are essential to sustain threatened ecological systems. These awaraness provide a quantitative framework for policymakers and conservation biologists to design effective intervations for wildlife protection and habitat restoration.

Introduction

In ecological systems, different species coexist and interact through relationships such as competition, cooperation, and predation, with prey-predator dynamics being a central theme (Sagamiko et al. 2021). The interactions between different species in an ecosystem can occur through various mechanisms such as predation, commensalism, competition, parasitism, and mutualism (Mapunda et al. 2018). However, many species face extinction threats due to different factors like over predation, toxicants, disease and environmental hazards

*Corresponding author: nuruyazidijuma@gmai.com
Received 25 Jul 2025; Revised 27 Sep 2025; Accepted 10 October 2025; Published 30 October 2025
https://doi.org/10.65085/2507-7961.1054

ISSN 0856-1761, e-ISSN 2507-7961

(Sagamiko et al. 2015). Toxicants in different ecosystems can emerge naturally or result from human activities, such as pesticide usage and industrialization, it has an impact on the long-term survival of prey and predator species and the overall biodiversity of the habitat (Lawaniya, 2018). Worldwide, numerous national parks and wildlife reserves have reported deaths due to toxicant exposure, while the specific causes of death vary by region and species, the impact of toxicants on wildlife populations is a global burning issue (Goswami et al. 2020). According to Ogada et al. (2015), over 150 vultures died in Serengeti National Park in Tanzania , significantly impacting the population of already vulnerable species. However, between 2010 and 2019, in Kaziranga National Park, India the park reported over 50 cases of wildlife deaths among rhinoceroses and elephants associated with toxicant exposure (Goswami et al. 2020). In Zimbabwe's Hwange National Park, over 300 elephants died in a mass poisoning event in 2013 after poachers laced waterholes with cyanide not only affected elephants but also indirectly killed numerous scavengers, including hyenas and vultures, that fed on the contaminated carcasses (Nguema 2016). In Kenya's Maasai Mara, a mass poisoning event killed 76 lions over a decade due to intentional bait poisoning by local communities (Ogada 2014). In North America, a rise in fox deaths has been reported due to the widespread use of rodenticides, which cause internal bleeding and eventual death (Riley et al., 2017). A study by Mateo (2009) reported over 30 deaths of bears foxes, lynxes and bears in Spanish parks including Donana National Park over 10-year period due to pesticide ingestion from contaminated prey. Diseases pose a significant threat to the ecosystem, affecting the growth and well-being of prey and predator species. They can be transmitted through various means, including predation, direct contact, and even through air in the environment (Pada Das et al. 2009). Numerous diseases impact the prey-predator system, such as tuberculosis, rabies, rift valley fever, rinderpest diseases, dengue disease, influenza, bird flu, anthrax, and canine distemper virus (Pada Das et al. 2009, Sagamiko et al. 2015, Borner 1995, Sinha 2009). In 2019, India's Kaziranga National Park lost several young elephants to EEHV, with over 25 cases recorded in the country (Kumara, 2020). Furthermore, a research conducted by the Tanzania Wildlife Research Institute in 2013 revealed that 10 percent of the investigated genus *Connochaetes* were found to be infected with Tuberculosis (MNRT Budget speech 2013). Additionally, in 2018, Namibia's Etosha National Park saw an anthrax outbreak that killed more than 50 zebras and 200 antelopes (Turner, 2020). Also in 2004, an anthrax outbreak in Queen Elizabeth National Park, Uganda, killed over 300 hippopotamuses in a few months, representing a significant loss for the population (Wafula 2008). Also, in 2014, an outbreak of CDV in China's Shaanxi province killed five pandas in the Qinling Mountains, a significant loss for this already endangered species (Xia 2014). Toxicants and diseases affect the survival of prey and predator species in an ecosystem. This necessitates the need of taking control measures to protect and sustain these species from extinction. Several studies have explored the effects of toxicants and diseases on prey-predator system. Khan and Samanta (2020) developed a mathematical model that integrates the effects of both toxicants and diseases on a Prey-predator system, focusing on how these two factors influence population dynamics over time. The model introduces Holling type-II functional response to depict the predator's feeding rate in response to prey density and examines the effects of toxicant accumulation and disease transmission. Additionally, Zhou et al. (2018) extended the Prey-predator model to consider the effects of both toxicants and diseases on the dynamics of the prey-predator system, incorporating a Holling type-III functional response. Various optimal control strategies have been widely examined to reduce the effects of toxicants and diseases in 2 prey-predator systems. For example, Numfor et al. (2017) investigated the impact of culling and biocontrol techniques on invasive predator

populations that pose a threat to native prey species. Their study developed an eco epidemiological model integrating both scalar and time-dependent controls, which accounted for the initial introduction of infected predators and continuous culling efforts. Similarly, Sahoo (2016) investigated disease management within predator-prey interactions by introducing alternative food sources for predators. This strategy was designed to alleviate predation on infected prey, thereby limiting the spread of disease. However, to the best of our knowledge, no study has incorporated the specific optimal control of the threats of toxicants and diseases to the survival of prey-predator systems in ecosystems. Therefore, this study focuses on formulating a generic prey-predator mathematical model considering the effects of both toxicants and diseases on the dynamics of the prey-predator system, incorporating a Holling type-I functional response. The suggested control efforts are bioremedial-antitoxic strategy for controlling toxicants and spatial isolation strategy for control of disease.

Materials and Methods

This section involves the formulation of models with threats and the one with time-dependent controls. Theoretical analysis of these models are also carried out.

Model development with threats

The model consists of prey population at time (t) denoted by $S(t)$ for susceptible prey, $I(t)$ for infected prey, $Y(t)$ for predator population, and $C(t)$ for the toxicant concentration in the environment. The dynamics of the species interaction is modelled using Holling type I functional response as the developed model is generic one that assumes a linear relationship between the predator's consumption rate and the prey population. The model is formulated under the following assumptions.

1. The prey population grows logistically with intrinsic growth rate r and environmental carrying capacity k.
2. The prey population consists of two Sub-classes, namely, the susceptible prey S(t) and the infected prey I(t).
3. Only the susceptible prey can reproduce. The logistic law is used to model the birth process with the assumption that births should always be positive
4. The infected prey is removed with death caused by disease at the rate e and by predation. However, both susceptible and infected prey contribute to the population density that determines logistic crowding toward the carrying capacity.
5. The disease is spread among the prey population only in order to avoid non-linearity of the model, while some of the infected prey undergo natural recovery λ. In ecological **predator–prey–disease models**, the type of disease that infects only the **prey population** (and not the predator) is usually referred to as a **host-specific disease** or a **prey-specific pathogen.** Examples of such diseases are Rabbit Hemorrhagic Disease Virus (RHDV) and Myxoma virus in rabbits (introduced in Australia).
6. Susceptible prey becomes infected when they come into contact with infected prey.
7. The predator population decreases due to natural death at the constant rate α.
8. The predation functional response of the predator towards susceptible and infected prey is modelled using a Holling type-I with predation rate coefficient N_1, and N_2. Consumed prey is converted into predator with efficiency L_1 and L_2.
9. Toxicant affects susceptible prey, infected prey and predator by reducing their survival and reproduction, δ represent toxicant induced mortality rate effect on susceptible prey, γ represent toxicant induced mortality rate effect on infected prey and β represents the toxicant-induced mortality rate in predators.

.

Under the forestated assumptions, the prey-predator mathematical model takes the following form using Holling type I functional response

$$\begin{aligned}
\frac{dS}{dt} &= rS\left(1 - \frac{S+I}{k}\right) - \mu SI + \lambda I - N_1 SY - \delta CS \\
\frac{dI}{dt} &= \mu SI - \lambda I - N_2 IY - eI - \gamma CI \\
\frac{dY}{dt} &= L_1 N_1 SY + L_2 N_2 IY - \alpha Y - \beta CY \\
\frac{dC}{dt} &= \delta CS + \gamma CI + \beta CY
\end{aligned} \qquad (1)$$

With the initial conditions:

$$S(0) = S_0 > 0, I(0) = I_0 \geq 0, Y(0) = Y_0 > 0, C(0) = C_0 > 0, N_1 > 0, N_2 > 0, 0 < L_1, L_2 \leq 1 \quad and \quad 0 < \delta, \gamma, \beta \leq 1$$

.

Where N_1 is the predation rate to the susceptible prey, N_2 is the predation rate to the infected prey and μ rate of transmission from Infected prey to Susceptible prey

Model analysis

The dynamic model (1) is analyzed to understand the dynamics of the diseases in the prey populations and toxicants in prey and predator populations.

Boundedness of the model

Theorem 1:

All solutions of the system (1) are uniformly bounded implies that the system is biologically valid and well behaved (Mukhopadhyay et al. (2009)).

Proof:

Assume *W* denote the total population in the ecosystem of the model under consideration, that is

$W = S + I + Y$ (2)

Differentiating both sides of equation (2) with respect to time *t* yields the following equation:

$$\frac{dW}{dt} = \frac{dS}{dt} + \frac{dI}{dt} + \frac{dY}{dt} \qquad (3)$$

Substituting the model equations (1) into (3) and simplifying, results to :

$$\begin{aligned}
\frac{dW}{dt} &\leq rS - eI - \alpha Y \\
&\leq S(r+1) - S - eI - \alpha Y \qquad (4) \\
&\leq S(r+1) - GW
\end{aligned}$$

Where $G = \min\{1, e, \alpha\}$

Then,

$$\frac{dW}{dt} + GW \leq S(r+1) \qquad (5)$$

Solving equation (5) and substituting the initial conditions of the model results to :

$$W \leq \frac{S(r+1)}{G} + e^{-(Gt+k)} \qquad (6)$$

As $t \to \infty$, equation (6) reduces to :

$$W \leq \frac{S(r+1)}{G} \quad (7)$$

Which implies that the solution is bounded for

$$0 \leq W \leq \frac{S(r+1)}{G} \quad (8)$$

Therefore, solutions *(S, I, Y)* of the model (1) in R_+^3 are confined to the region

$$\sigma = \left\{ (S,I,Y) \in R_+^3 : W \leq \frac{S(r+1)}{G} + \varepsilon \right\} \forall \varepsilon > 0 \ as \ t \to \infty \quad (9)$$

Boundedness of the concentration of toxicants

Proof:

$$\frac{dC}{dt} = C(\delta S + \gamma I + \beta Y) \quad (10)$$

Since *S, I, Y* are assumed to be bounded, there exist a positive constant *M* such that: $S + I + Y \leq M$. Let: $K = Max(\delta, \gamma, \beta)$, so that

$\delta S + \gamma I + \beta Y \leq K(S + I + Y) \leq KM$

From the limit $0 < \delta, \gamma, \beta \leq 1$, we assume that $\delta = \gamma = \beta = 1$.Thus, the equation satisfies:

$$\frac{dC}{dt} \leq KMC$$

By solving differential inequality, the solution will be $C(t) \leq C(0)e^{K}Mt$ Since exponential growth is bounded for finite *t*, this confirms that *C (t)* remains finite for all $t \leq 0$ then the Toxicant concentration *C* is bounded (Sinha et al. 2009).

Positivity of solutions

Theorem 2:

Let $S(0) > 0, I(0) > 0, Y(0) > 0, C(0) > 0$. *This implies that the solutions for* $S(t), I(t), Y(t) and C(t)$ *of the model (3.1) are positive* $\forall t > 0$ *(Hugo et al, 2012).*

Proof:

Let $S(t), I(t), Y(t)$ and $C(t)$ be any solution of system (1). Assuming that one solution of the system (1) is at least not positive, then the following cases occur: (Brauer and Castillo-Chavez 2001, Brauer and Castillo-Chavez 2012)

1. There exists t_1, such that
   $S(0) > 0, S(t_1) = 0, S'(t_1) < 0, I(t) > 0, Y(t) > 0, C(t) > 0, 0 \leq t < t_1$.
2. There exists t_2, such that
   $I(0) > 0, I(t_2) = 0, I'(t_2) < 0, S(t) > 0, Y(t) > 0, C(t) > 0, 0 \leq t < t_2$.
3. There exists t_3, such that
   $Y(0) > 0, Y(t_3) = 0, Y'(t_3) < 0, I(t) > 0, S(t) > 0, C(t) > 0, 0 \leq t < t_3$.
4. There exists t_4, such that
   $C(0) > 0, C(t_4) = 0, C'(t_4) < 0, I(t) > 0, S(t) > 0, Y(t) > 0, 0 \leq t < t_4$.

If case (1) holds, then we obtain; $S'(t_1) = \lambda I > 0$ This contradicts $S'(t_1) < 0$.

If case (2) holds, then we obtain; $I'(t_2) = 0$. This contradicts $I'(t_2) < 0$.

If case (3) holds, then we obtain; $Y'(t_3) = 0$. This contradicts $Y'(t_3) < 0$.

If case (4) holds, then we obtain; $C^{'}(t_4)=0$. This contradicts $C^{'}(t_4)<0$.
From the arbitrariness of $S(t)$, $I(t)$, $Y(t)$ and $C(t)$ all solutions of the system (1) remain positive $\forall t>0$.

Equilibrium points
The equilibrium points of model equation (1) are obtained by setting:

$$\frac{dS}{dt}=\frac{dI}{dt}=\frac{dY}{dt}=\frac{dC}{dt}=0 \quad (11)$$

Therefore, the model equations (1) has the following equilibrium points:

1. The axial equilibrium $E_1(S^*,I^*Y^*C^*)=(k,0,0,0)$, where the predator and infected prey population die out while leaving susceptible prey to growth to its carrying capacity with no toxicants.
2. The equilibrium point where the disease eventually disappears from the prey population with absence of predator is denoted by E_2 as : $(S^*,I^*Y^*C^*)=E_2(0,0,0,C)$
3. The equilibrium points where both toxicants and diseases eventually disappear from the prey-predator population is denoted by E_3 as:

$$(S^*,I^*Y^*C^*)=E_3\left(\frac{\alpha}{L_1N_1},0,rN_1-\frac{r\alpha}{L_1k},0\right).$$

4. The equilibrium points where the predator population dies out and toxicants eliminated from the prey predator system is denoted by E_4 as:

$$(S^*,I^*Y^*C^*)=E_4\left(\frac{e+\lambda}{\mu},\frac{rkS-rS^2}{ke+rS},0,0\right).$$

Local stability analysis: Using the system of equations of model (1) the general Jacobian matrix of the equations is given by:

$$J_E=\begin{bmatrix}\frac{\partial g_1}{\partial S} & \frac{\partial g_1}{\partial I} & \frac{\partial g_1}{\partial Y} & \frac{\partial g_1}{\partial C}\\ \frac{\partial g_2}{\partial S} & \frac{\partial g_2}{\partial I} & \frac{\partial g_2}{\partial Y} & \frac{\partial g_2}{\partial C}\\ \frac{\partial g_3}{\partial S} & \frac{\partial g_3}{\partial I} & \frac{\partial g_3}{\partial Y} & \frac{\partial g_3}{\partial C}\\ \frac{\partial g_4}{\partial S} & \frac{\partial g_4}{\partial I} & \frac{\partial g_4}{\partial Y} & \frac{\partial g_4}{\partial C}\end{bmatrix}$$

where

$$g_1(S,I,Y,C)=\frac{dS}{dt},g_2(S,I,Y,C)=\frac{dI}{dt},g_3(S,I,Y,C)=\frac{dY}{dt}\text{ and }g_4(S,I,Y,C)=\frac{dC}{dt}$$

.
This gives

$$J_E = \begin{bmatrix} A & \frac{rS}{k} - \mu S + \lambda & -N_1 S & -\delta S \\ \mu I & B & -N_2 I & -\gamma I \\ L_1 N_1 Y & L_2 N_2 Y & R & -\beta Y \\ \delta C & \gamma C & \beta C & D \end{bmatrix}$$

where,

$$A = r - \frac{2rS}{k} - \frac{rI}{k} - \mu I - N_1 Y - \delta C,$$

$$B = \mu S - \lambda - N_2 Y - e - \gamma C,$$

$$R = L_1 N_1 S + L_2 N_2 I - \alpha - \beta C$$

and

$$D = \delta S + \gamma I + \beta Y$$

Theorem 3:

The axial equilibrium $E_1(S^*, I^* Y^* C^*) = (k,0,0,0)$ *is locally asymptotically stable if* $\mu k < e + \lambda, kL_1 N_1 < \alpha \psi_1$ *and* $\delta k < 0.$

Proof:

The Jacobian matrix evaluated at the axial equilibrium point E_1 is given by:

$$J(E_1) = \begin{bmatrix} -r & r - \mu k + \lambda & -N_1 k & -\delta k \\ 0 & \mu k - e - \lambda & 0 & 0 \\ 0 & 0 & kL_1 N_1 - \alpha & 0 \\ 0 & 0 & 0 & \delta k \end{bmatrix}$$

The eigenvalues for the Jacobian matrix $J(E_1)$ are

$\psi_1 = -r, \psi_2 = k\mu - e - \lambda, \psi_3 = kL_1 N_1 - \alpha$ *and* $\psi_4 = \delta k$

Then, for stability, we need to have:

$\psi_2 < 0,$ *if* $k\mu - e - \lambda < 0,$ by rearranging result to $k\mu < e + \lambda$

$\psi_3 < 0,$ *if* $kL_1 N_1 - \alpha < 0,$ by rearranging result to $kL_1 N_1 < \alpha$

$\psi_4 < 0,$ *if* $k\delta < 0$

This means that if feeding efficiency of predator is low such that $kL_1 N_1 < \alpha$ and interaction of infected prey population and susceptible prey population is less than the total number of recovery (λ) and death of prey due to diseases (e) then the predator species will extinct and prey population will reach its carrying capacity k (Hugo and Simanjilo 2019).

Theorem 4:

The equilibrium point; $E_2(0,0,0,C)$ *where the disease eventually disappears from the prey population with absence of predator, is locally asymptotically stable if* $C\delta > r.$

Proof:

The Jacobian matrix of system (1) at the equilibrium point E_2 is given by:

$$J(E_2) = \begin{bmatrix} r - \delta C & \lambda & 0 & 0 \\ 0 & -\lambda - e - \gamma C & 0 & 0 \\ 0 & 0 & -\alpha - \beta C & 0 \\ \delta C & \gamma C & \beta C & 0 \end{bmatrix}$$

The eigenvalues for the Jacobian matrix $J(E_2)$ are

$\psi_1 = 0, \psi_2 = -\alpha - \beta C, \psi_3 = r - \delta C$ and $\psi_4 = -\lambda - e - \gamma C$

Then, for stability, we need to have:

$r - \delta C < 0,$ requires while zero eigenvalue means the system is at least marginally stable or Lyapunov stable.

Theorem 5:

The equilibrium point; $E_3\left(\frac{\alpha}{L_1 N_1}, 0, rN_1 - \frac{r\alpha}{L_1 k}, 0\right)$ *where both toxicants and diseases eventually disappear from the prey-predator population is locally asymptotically stable when* $k < \frac{N_1 \alpha \beta r}{\alpha\delta + L_1 N_1^2 \beta r}$.

Proof:

The Jacobian matrix of system (1) at the equilibrium point E_3 is given by:

$$J(E_3) = \begin{bmatrix} r - \frac{2r\alpha}{kL_1N_1} - N_1^2 r + \frac{r\alpha N_1}{kL_1} & \frac{k\lambda L_1 N_1 - k\mu\alpha + r\alpha}{kL_1 N_1} & \frac{-\alpha}{L_1} & \frac{-\delta\alpha}{L_1 N_1} \\ 0 & \frac{N_1 N_2 \alpha r + k\mu\alpha}{kL_1 N_1} - \lambda - rN_1 N_2 - e & 0 & 0 \\ \frac{kL_1^2 N_1^2 r - \alpha r L_1 N_1}{kL_1} & \frac{L_2 N_2 kL_1 N_1 r - \alpha r L_2 N_2}{kL_1} & 0 & \frac{-\beta r k L_1 N_1 + \beta r\alpha}{kL_1 N_1} \\ 0 & 0 & 0 & \frac{\delta\alpha}{L_1 N_1} + W \end{bmatrix}$$

The eigenvalues for the Jacobian matrix $J(E_3)$ are:

$$\psi_1 = \frac{-L_1 N_1^2 N_2 kr - L_1 N_1 ek - L_1 N_1 \lambda k - N_1 N_2 \alpha r - \alpha k\mu}{L_1 N_1 k},$$

$$\psi_2 = \frac{-L_1 N_1^3 kr - L_1 N_1 kr - N_1^2 \alpha r - 2\alpha r - \sqrt{\Delta}}{2L_1 N_1 k},$$

$$\psi_3 = \frac{-L_1 N_1^3 kr - L_1 N_1 kr - N_1^2 \alpha r - 2\alpha r - \sqrt{\Delta}}{2L_1 N_1 k},$$

$$\psi_4 = \frac{L_1 N_1^2 \beta kr - N_1 \alpha\beta r + \alpha\delta k}{L_1 N_1 k}$$

where

$$\Delta = L_1^2 N_1^6 k^2 r^2 - 4L_1^2 N_1^4 \alpha k^2 r - 2L_1^2 N_1^4 k^2 r^2 + L_1^2 N_1^2 k^2 r^2 - 2L_1 N_1^5 \alpha k r^2 + 4L_1 N_1^3 \alpha^2 k r + 6L_1 N_1^3 \alpha k r^2 - 4L_1 N_1 \alpha k r^2 + N_1^4 \alpha^2 r^2 - 4N_1^2 \alpha^2 r^2 + 4\alpha^2 r^2$$

and

$$W = \frac{\beta r k L_1 N_1 - \beta \alpha r}{k L_1}$$

Then, for stability, we need to have;

$L_1 N_1^2 \beta k r - N_1 \alpha \beta r + \alpha \delta k < 0$, upon re-arrangement results to $k < \frac{N_1 \alpha \beta r}{\alpha \delta + L_1 N_1^2 \beta r}$.

Theorem 6:

The boundary equilibrium point; $E_4 = \left(\frac{e+\lambda}{\mu}, \frac{rkS - rS^2}{ke + rS}, 0, 0 \right)$ *where predator dies out and toxicants eventually disappears from the prey-predator population is locally asymptotically stable if* $k < S$ *and* $e < -\lambda$.

Proof:

The Jacobian matrix of system (1) at the equilibrium point E_4 is given by:

$$J(E_4) = \begin{bmatrix} r - \frac{2rD}{k} - \frac{rA}{k} - \mu A & \frac{rD}{k} - e & -N_1 D & -\delta D \\ \mu A & 0 & -N_1 A & -\gamma A \\ 0 & 0 & L_2 N_2 A + L_1 N_1 D - \alpha & 0 \\ 0 & 0 & 0 & \gamma A + \delta D \end{bmatrix}$$

where by $A = \frac{-rS^2 + rkS}{ke + rS}$ and $D = \frac{e+\lambda}{\mu}$

The eigenvalues for the Jacobian matrix $J(E_4)$ are;

$$\psi_1 = L_2 N_2 A + L_1 N_1 D - \alpha, \quad \psi_2 = \frac{-(\mu A k + 2rD - rk - F)}{2k}, \quad \psi_3 = \frac{\mu A k + 2rD - rk - F}{2k}$$

and $\psi_4 = \gamma A + \delta D$

where,

$$F = \sqrt{\left(\begin{array}{l} A^2 k^2 \mu^2 + 2A^2 k \mu r + 8ADkr\mu - 4Aek^2 \mu - 2Ak^2 \mu r + \\ A^2 r^2 + 4ADr^2 - 2Akr^2 + 4D^2 r^2 - 4Dkr^2 + k^2 r^2 \end{array} \right)} \qquad (12)$$

Then, for stability we need to have:

$\gamma A + \delta D < 0$, since $A = \frac{-rS^2 + rkS}{ke + rS}$ and $D = \frac{e+\lambda}{\mu}$. Hence; $k < S$ and $e < -\lambda$ satisfy the stability condition. From $L_2 N_2 A + L_1 N_1 D - \alpha < 0$, $A = \frac{-rS^2 + rkS}{ke + rS}$ and $D = \frac{e+\lambda}{\mu}$ then $k < S$ and $e < -\lambda$ satisfy the stability condition.

Global stability analysis

The global stability analysis of the system (1) is performed around positive equilibrium point $E(S^*, I^*Y^*C^*)$ of coexistence by using the theorem of Lyapunov function *U*(Hugo and Simanjilo 2019).

Theorem 7 :

If; $$U = \frac{1}{2}(S - S^*)^2 + \frac{1}{2}\mu_1(I - I^*)^2 + \frac{1}{2}\mu_2(Y - Y^*)^2 + \frac{1}{2}\mu_3(C - C^*)^2 \quad (13)$$

Where $\mu_1, \mu_2, \mu_3 > 0$ *are to be carefully chosen such that* $U'(E) = 0$ *then* $E(S^*, I^*Y^*C^*)$ *and* $U = (S, I, Y, C) > 0 \ \forall S, I, Y, C / \{E\}$. *If the time derivatives of U is* $\frac{dU}{dt} \leq 0, \ \forall S, I, Y, C \in \xi$. *Then it follows that* $\frac{dU}{dt} = 0, \ \forall S, I, Y, C \in \xi$ *implies that* E^* *of the system is Lyapunov stable and* $\frac{dU}{dt} \leq 0, \ \forall S, I, Y, C \in \xi$ *near* E^* *is globally stable.*

Proof:

$$\frac{dU}{dt} = (S - S^*)\frac{dS}{dt} + \mu_1(I - I^*)\frac{dI}{dt} + \mu_2(Y - Y^*)\frac{dY}{dt} + \mu_3(C - C^*)\frac{dC}{dt} \quad (14)$$

Substituting the model equations (1) to (14) results to:

$$\begin{aligned}\frac{dU}{dt} &= (S - S^*)\left(rS\left(1 - \frac{S + I}{k}\right) - \mu SI + \lambda I - N_1 SY - \delta CS\right) \\ &+ \mu_1(I - I^*)(\mu SI - \lambda I - N_2 IY - eI - \gamma CI) \\ &+ \mu_2(Y - Y^*)(L_1 N_1 SY + L_2 N_2 IY - \alpha Y - \beta CY) \\ &+ \mu_3(C - C^*)(\delta CS + \gamma CI + \beta CY)\end{aligned} \quad (15)$$

Then, equation (15) becomes:

$$\begin{aligned}\frac{dU}{dt} &= (S - S^*)\left(r\left(1 - \frac{S + I}{k}\right) - \mu I + \frac{\lambda I}{S} - N_1 Y - \delta C\right)(S - S^*) \\ &+ \mu_1(I - I^*)(\mu S - \lambda - N_2 Y - e - \gamma C)(I - I^*) \\ &+ \mu_2(Y - Y^*)(L_1 N_1 S + L_2 N_2 I - \alpha - \beta C)(Y - Y^*) \\ &+ \mu_3(C - C^*)(\delta S + \gamma I + \beta Y)(C - C^*)\end{aligned} \quad (16)$$

Rearranging equation (16) leads to :

$$\begin{aligned}\frac{dU}{dt} &= -(S - S^*)^2\left(r\left(-1 + \frac{S + I}{k}\right) + \mu I - \frac{\lambda I}{S} + N_1 Y + \delta C\right) \\ &- \mu_1(I - I^*)^2(-\mu S + \lambda + N_2 Y + e + \gamma C) \\ &- \mu_2(Y - Y^*)^2(-L_1 N_1 S - L_2 N_2 I + \alpha + \beta C) \\ &- \mu_3(C - C^*)^2(-\delta S - \gamma I - \beta Y)\end{aligned} \quad (17)$$

Assuming all parameter with negative sign belong to a certain constant. Thus, it is possible to set $\mu_1, \mu_2, \mu_3 > 0$ such that $U'(E) \leq 0$ an endemic positive equilibrium point is globally stable.

The Model with Time Dependent Control Effort

Time dependent control efforts on bioremedial-antitoxic strategy $u_2(t)$ and spatial isolation strategy $u_1(t)$ as controls to curtail the threats to the prey-predator system are introduced into model (1). The dynamics are formulated as an optimal control with the following assumptions. The control rate of diseases through spatial isolation strategy u_1 lies in the range $0 \le u_1 \le 1$, the control rate of toxicants through a Bioremedial-Antitoxic strategy u_2 lies in the range $0 \le u_2 \le 1$. It is assumed that susceptible prey populations have been infected at the rate $(1-u_1)\mu SI$ while others remain in the susceptible class. Then, the control rate through spatial isolation strategy of infected and susceptible prey $u_1(t)$ varies with time and it will be at the optimal level whenever $u_1(t)=1$ and less effective when $u_1(t)=0$. Also it is assumed that the infected prey, susceptible prey and predator population will be controlled from toxicants through the Bioremedial-Antitoxic strategy $u_2(t)$ at a rate of $(1-u_2)$ and it will be at the optimal level whenever $u_2(t)=1$ and less effective when $u_2(t)=0$.

The modified model (1) by incorporating time-dependent control is given by:

$$\begin{aligned}
\frac{dS}{dt} &= rS\left(1-\frac{S+I}{k}\right)-(1-u_1)\mu SI+\lambda I-N_1SY-(1-u_2)\delta CS\\
\frac{dI}{dt} &= (1-u_1)\mu SI-\lambda I-N_2IY-eI-(1-u_2)\gamma CI\\
\frac{dY}{dt} &= L_1N_1SY+L_2N_2IY-\alpha Y-(1-u_2)\beta CY\\
\frac{dC}{dt} &= (1-u_2)(\delta CS+\gamma CI+\beta CY)
\end{aligned} \tag{18}$$

The control boundedness must satisfy the Lebesgue measurable control as:

$U=\{u=(u_1,u_2), 0 \le u_i \le u_i \max, i=1,2\}$.

The intention is to minimize the spread of diseases through interaction among prey populations, and also to minimize number of prey-predator populations affected by toxicants through the following objective function J.

Min of (u_1,u_2) such that, $J=\int_0^T \left(BI+D(S+I+Y+C)+\frac{1}{2}A_1u_1^2+\frac{1}{2}A_2u_2^2\right)dt$,

where T is the final time of control, BI is the cost associated with the spatial isolation strategy of preys and $D(S+I+Y+C)$ is the cost associated with the controlling toxicants to both populations, while A_1 and A_2 are relative cost weight for each individual control measure. The objective function involved in minimizing the number of population affected by toxicants and infected prey. We apply quadratic function in the objective function as it satisfies the optimality conditions (Massawe et al. 2015, Okosun et al. 2013). Then the optimal controls $u_1^*(t)$ and $u_2^*(t)$ exist such that:

$J(u_1^*(t),u_2^*(t))=\min\{J(u_1(t),u_2(t)):u_1(t),u_2(t)\in U\}$

Where

$U=\{u_1(t),u_2(t)\}$ are measurable, $0 \le (u_1(t),u_2(t)) \le 1$ for $t \in [0,T]$

The necessary conditions for Pontryagin's Maximum principle (Lenhart et al., 2007)) need to be satisfied with the formulated model, usually converts the system of equation (18) and objective functional *J* into a problem of minimizing point-wise a Hamiltonian *(H)*, with respect to $u_1(t)$, $u_2(t)$ as:

$$\begin{aligned} H &= BI + D(S+I+Y+C) + \frac{1}{2}A_1u_1^2 + \frac{1}{2}A_2u_2^2 + \\ &+ \tau_1\left(rS\left(1-\frac{S+I}{k}\right) - (1-u_1)\mu SI + \lambda I - N_1SY - (1-u_2)\delta CS\right) \\ &+ \tau_2((1-u_1)\mu SI - \lambda I - N_2IY - eI - (1-u_2)\gamma CI) \\ &+ \tau_3(L_1N_1SY + L_2N_2IY - \alpha Y - (1-u_2)\beta CY) \\ &+ \tau_4((1-u_2)(\delta CS + \gamma CI + \beta CY)) \end{aligned} \quad (19)$$

where τ_i, $i=1,2,3,4$ are the co-state variables associated by S, *I, Y, C.* The adjoint equations are obtained by:

$$\frac{d\tau_i}{dt} = -\frac{\partial H}{\partial i} \quad (20)$$

with transversality condition:

$$\tau_i(T) = 0 \quad (21)$$

From (19) we obtain the following adjoint equations.

$$\begin{aligned} \frac{\partial H}{\partial S} &= -D - \tau_1 r\left(1-\frac{S+I}{k}\right) + \frac{\tau_1 rS}{k} + \tau_1(1-u_1)\mu I + \tau_1 N_1 Y + \tau_1(1-u_2)\delta C \\ &- \tau_2(1-u_1)\mu I - \tau_3 L_1 N_1 Y - \tau_4(1-u_2)\delta C \\ \frac{\partial H}{\partial I} &= -B - D + \frac{\tau_1 rS}{k} + \tau_1(1-u_1)\mu S - \tau_1\lambda - \tau_2(1-u_1)\mu S + \tau_2\lambda + \tau_2 N_2 Y \\ &+ \tau_2 e + \tau_2(1-u_2)\gamma C - \tau_3 L_2 N_2 Y - \tau_4(1-u_2)\gamma C \\ \frac{\partial H}{\partial Y} &= -D + \tau_1 N_1 S + \tau_2 N_2 I - \tau_3 L_1 N_1 S - \tau_3 L_2 N_2 I + \tau_3\alpha + \tau_3(1-u_2)\beta C - \tau_4(1-u_2)\beta \\ \frac{\partial H}{\partial C} &= -D + \tau_1(1-u_2)\delta S + \tau_2(1-u_2)\gamma I + \tau_3(1-u_2)\beta Y - \tau_4(1-u_2)\delta S - \tau_4(1-u_2)\gamma I - \tau_4(1-u_2)\beta Y \end{aligned} \quad (22)$$

The optimality of the control problem is obtained by:

$$u_i^*(t) = \frac{\partial H}{\partial u_i} \quad (23)$$

Thus,

$\frac{\partial H}{\partial u_i} = 0$. Then,

$u_1(t)$ and $u_2(t)$ are solved at $u_i^*(t) \in [0,1]$.

where *i = 1,2*. The solution of $u_1^*(t)$ and $u_2^*(t)$ are presented in a compact form as:

$$u_1^*(t) = \max\left[0, \min\left(1, \frac{\mu\tau_2 SI - \mu\tau_1 SI}{u_1 A_1}\right)\right]$$

and

$$u_2^*(t) = \max\left[0,\ \min\left(1, \tau_4\beta CY + \tau_4\beta CI + \tau_4\delta CS - \tau_3\beta CY - \tau_2\beta CI - \tau_1\delta CS - u_2 A_2\right)\right].$$

Numerical Results

These results are based on simulations of classical model and the model with controls

Simulation of the classical model (Results).

The numerical solution of the optimal control model have been determined using the Forward-Backward sweep method as the dynamics of the model based on continuous time. Also the fourth order Runge Kutta method have been involved(Hugo and Simanjilo, 2019) Fourth order Runge Kutta method is chosen because the convergence under this method is higher due to higher degree of accuracy and widely used in studies that involve optimal control problems

Table 1 : Parameter value used in numerical simulation.

Parameter	Value (Number)	Source
r	11.2	Mukhopadhyay and Bhattacharyya 2009
k	200	Assumed
μ	1.2	Mukhopadhyay and Bhattacharyya 2009
δ	0.1	Assumed
λ	0.1	Sinha et al 2009
N_1	0.4	Hugo et al 2012
γ	0.5	Assumed
N_2	0.8	Hugo and Simanjilo 2019
β	0.4	Assumed
e	0.01	Hugo and Simanjilo 2019
L_1	0.025	Assumed
L_2	0.05	Assumed
α	0.6	Hugo and Simanjilo 2019

The numerical simulations resulted into the following Figures:

i. Dynamics of the susceptible prey and infected prey populations when they interact in the system.

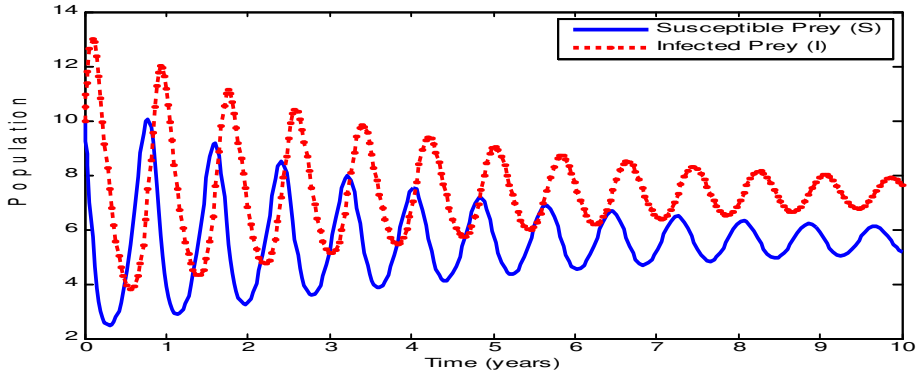

Figure 1: Effects of Prey species interactions as a result of disease transmission.

Figure 1 shows how susceptible prey population interact with infected prey population in the presence of diseases, the changes in population sizes of both susceptible and infected prey population occur, as the disease transmission rate increases the susceptible prey population decreases, also as the mortality rate *(e)* of

infected prey population increases the population of infected prey decreases, furthermore the increase of recovery rate of infected prey population tend to reduce infected prey population and increases the susceptible prey population. The population of infected prey and susceptible prey decreased toward extinction if diseases are not controlled.

ii. The interaction between susceptible prey population, infected prey population and predator population.

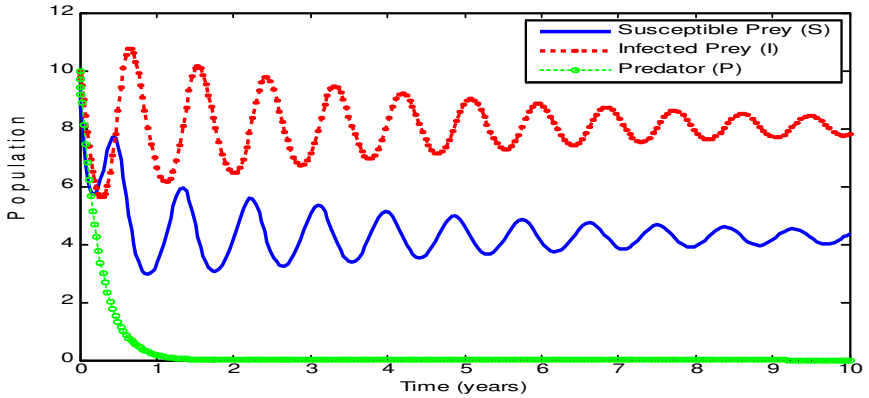

Figure 2: Effects of interaction between predator and prey populations

Figure 2 shows that in the prey–predator system, disease causes susceptible prey to become infected over time, leading to a decline in the susceptible class and an increase in the infected class. However, as the recovery rate (λ) rises, more infected prey return to the susceptible group, boosting its population. If the disease remains uncontrolled, both susceptible and infected prey eventually go extinct, which in turn drives the predator population to collapse due to food scarcity.

iii. The effects of toxicants to the prey-predator populations system.

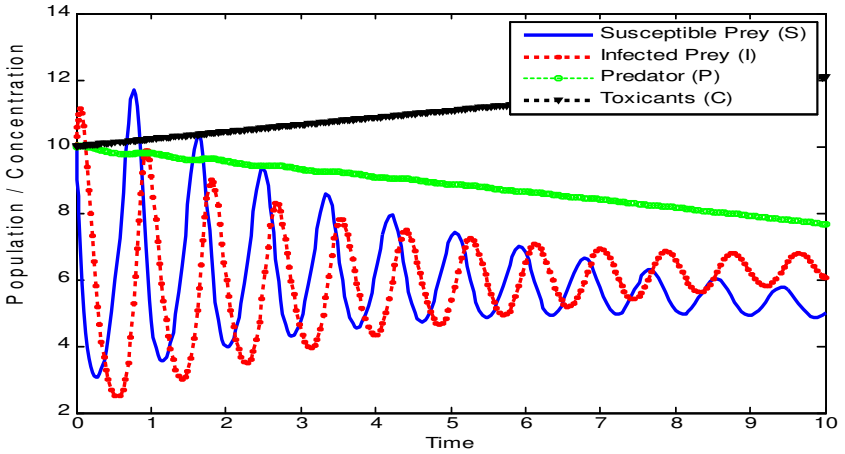

Figure 3: Effects of toxicants on the prey-predator populations

Toxicants affects the health of infected prey population, susceptible prey population and predator population leading to higher mortality rates. It is evident from Figure 3 that as the rate of toxicants increases the level of population of prey and predator species decreases.

Numerical Simulation for Optimal Control Analysis

Three types of strategies are to be considered, these include the control rate by applying only spatial isolation strategy, through bioremedial-antitoxic strategy and the combination of the two strategies.

Control by applying spatial isolation strategy

i. Application of spatial isolation control strategy to the susceptible prey population.

The application of spatial isolation u_1 is used to optimize the objective function J while bioremedial-antitoxic strategy u_2 equal to zero.

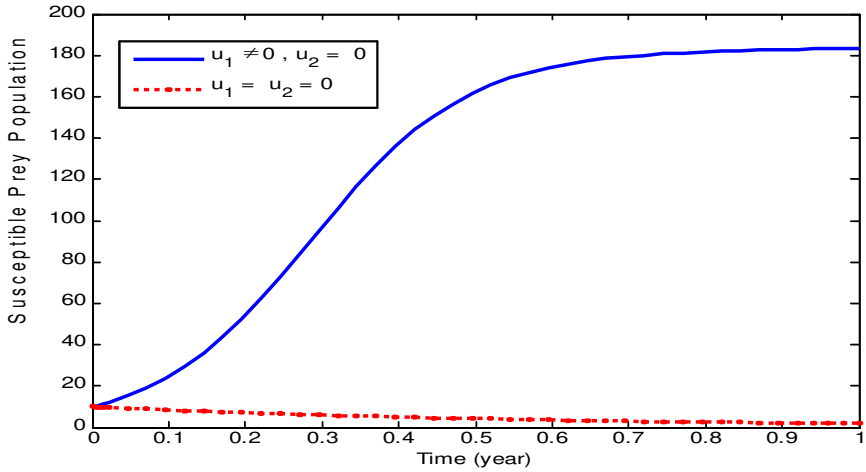

Figure 4: Effects of spatial isolation strategy on the susceptible prey population.

Figure 4, demonstrated that applying spatial isolation strategy to susceptible prey population reduces the disease transmission rate, before introducing control of spatial isolation strategy, the results show that susceptible prey population undergo extinction as portrayed by red dotted curve. After introducing the control of spatial isolation strategy to susceptible prey population increased toward carrying capacity at final time of control as portrayed by blue curve.

Application of spatial isolation control strategy to the infected prey populations.

The application of spatial isolation strategy u_1 is used to optimize the objective function J while bioremedial-antitoxic strategy u_2 equal to zero.

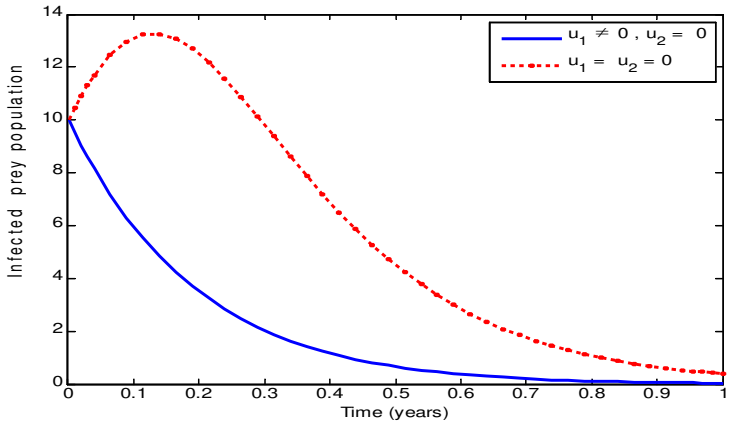

Figure 5: Effects of spatial isolation strategy on infected prey population.

In Figure 5, before introducing spatial isolation control strategy the number of infected prey population increased, later on infected prey population began to decrease until reaching zero due to the mortality rate *(e)*, recovery rate (λ), predation rate (N_2) and toxicants mortality rate (γ). When spatial isolation strategy was introduced, infected prey population decreased directly to zero, indicating that the disease has been eliminated from the system.

Control through bioremedial-antitoxic strategy

i. Application of bioremedial-antitoxic control strategy to the predator populations.

The application of bioremedial-antitoxic strategy u_2 is used to optimize the objective function J while spatial isolation strategy u_1 equal to zero.

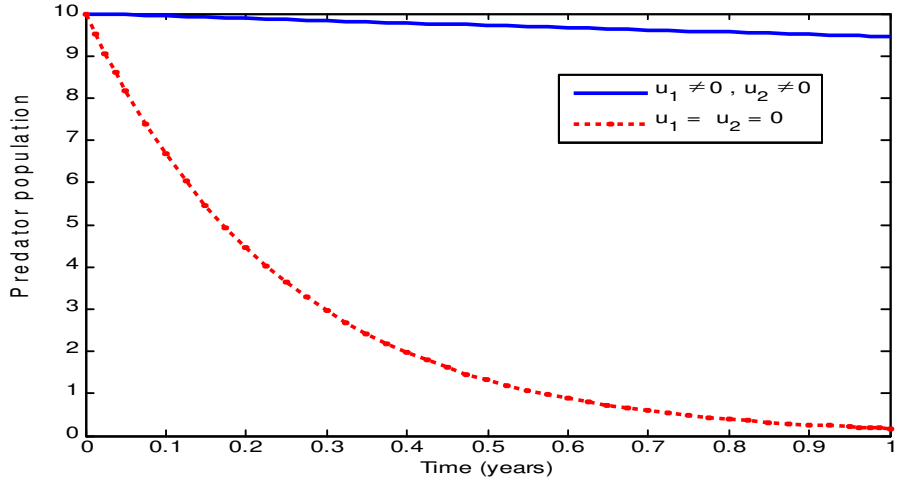

Figure 6: Effects of bioremedial-antitoxic strategy on the dynamics of predator population.

From Figure 6, before introducing bioremedial-antitoxic control strategy, the predator population decreased drastically due to effect of toxicants and natural death.

Introduction of bioremedial-antitoxic control strategy maintained the level of predator population while the slight decrease as portrayed by the blue curve is due to natural death (α).

ii. Application of bioremedial-antitoxic control strategy on the throwing toxicant packets into the environment.

The application of bioremedial-antitoxic strategy u_2 a is used to optimize the objective function J while spatial isolation strategy u_1 equal to zero.

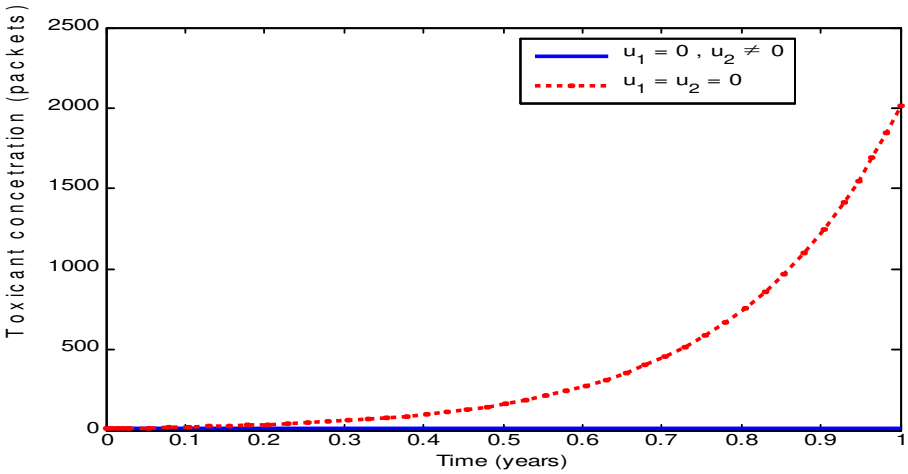

Figure 7: Effects of bioremedial-antitoxic strategy on the concentration of toxicants

Figure 7, illustrates a significant variation in toxicant concentration before and after control measures. This phenomena demonstrates that effective bioremedial-antitoxic strategy reduces the concentration of toxicants in the ecosystem. Before implementing control measures to prevent toxicants in the environment, the toxicant levels increased rapidly over time as shown by the red dotted curve. However, after implementing control measures, the toxicant levels were fully regulated and gradually disappeared from the environment, reaching to concentration of zero as the control period progressed, as indicated by the blue curve.

iii. Application of bioremedial-antitoxic control strategy to the susceptible prey populations.

The application of bioremedial-antitoxic strategy u_2 is used to optimize the objective function J while spatial isolation u_1 equal to zero.

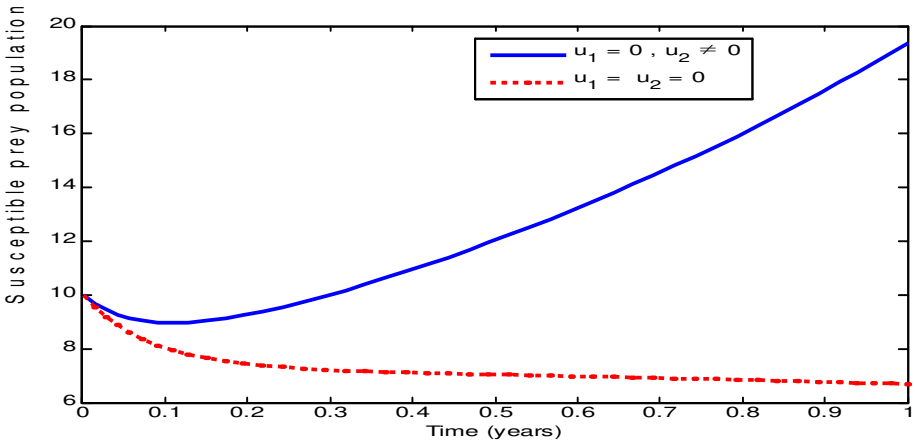

Figure 8: Effects of bioremedial-antitoxic strategy on the susceptible prey population.

Figure 8 provides clear evidence on how susceptible prey populations change before and after bioremedial-antitoxic control strategy. Before control the number of susceptible prey population decline towards extinction over time, as indicated by the red dotted curve. However, after implementing the control measures, the population initially decreased after sometimes susceptible prey population increased rapidly as indicated by the blue curve.

iv. Application of bioremedial-antitoxic control strategy to the infected prey populations.

The application of bioremedial-antitoxic strategy u_2 is used to optimize the objective function J while spatial isolation u_1 equal to zero.

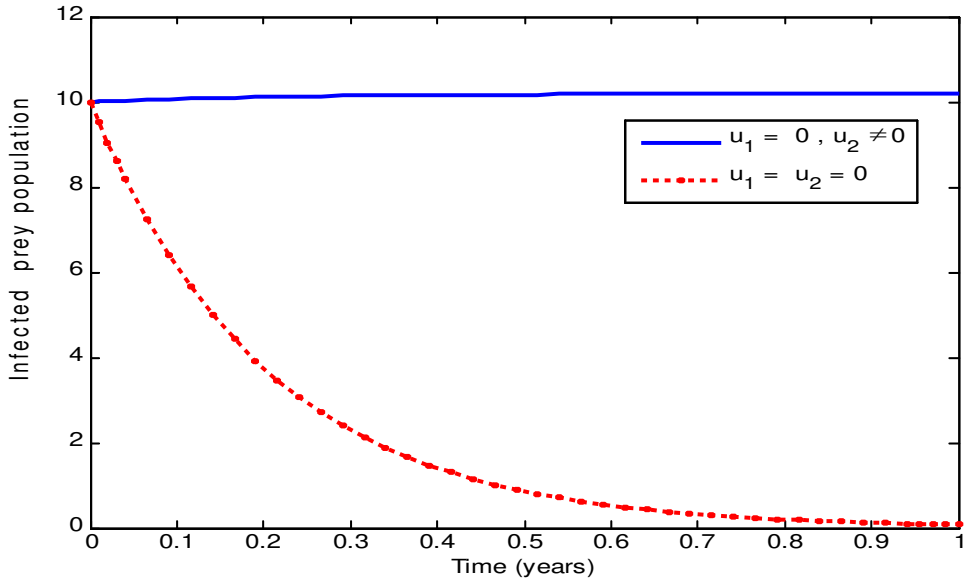

Figure 9: Effects of bioremedial-antitoxic strategy on infected prey population.

Figure 9 illustrates the dynamics of infected prey population before and after the implementation of bioremedial-antitoxic strategy control measures. Prior to

bioremedial-antitoxic strategy control measure as indicated by the red dotted curve, the population declines towards extinction over time. However, after the implementation of control measures, the population gradually increases, as shown by the blue curve.

Control rate by applying both spatial isolation and bioremedial-antitoxic strategies

i. Control rate by applying both spatial isolation and bioremedial-antitoxic strategies on the concentration of toxicant in the prey-predator system.

Both application of spatial isolation u_2 and bioremedial-antitoxic strategy u_1 are used to optimize the objective function *J.*

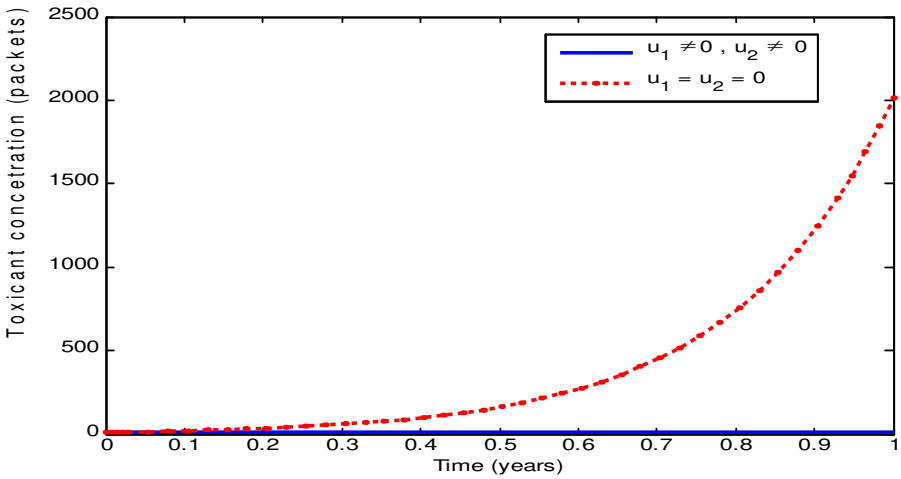

Figure 10: Effect of application of spatial isolation and bioremedial-antitoxic strategies on the concentration of toxicants.

The results of Figure10, after applying control strategies spatial isolation and bioremedial-antitoxic on the accumulation of toxicants in the environment, the results are the same as the ones portrayed by Figure 7, which were obtained by applying only bioremedial-antitoxic control strategy to control toxicants. This means that spatial isolation has no significant impact on preventing toxicants in the environment.

ii. Control rate by applying both spatial isolation and bioremedial-antitoxic strategies to the predator population.

Both application of spatial isolation u_1 and bioremedial-antitoxic u_2 are used to optimize the objective function *J.*

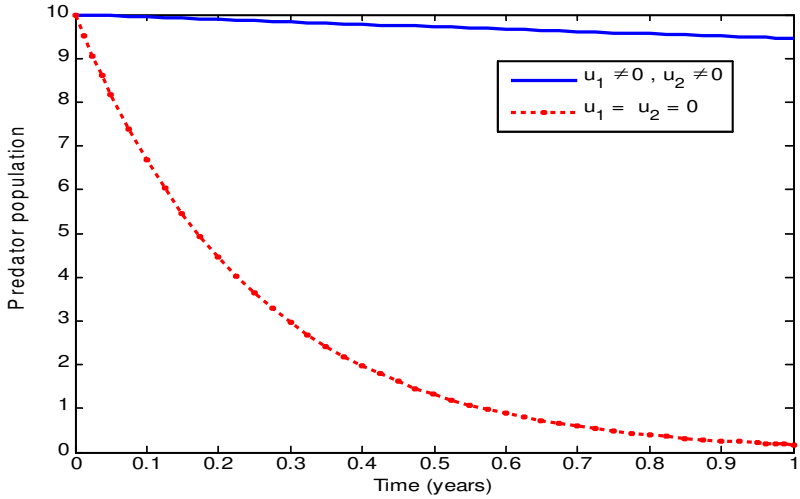

Figure 11: Effect of spatial isolation and bioremedial-antitoxic strategies on the predator population.

In Figure 11, results show effects of application of both control strategies spatial isolation and bioremedial-antitoxic to the predator population. After applying spatial isolation and bioremedial-antitoxic strategies as the control measures on the predator population(Refer Figure 11), the obtained results do not differ with the results of Figure 6, which were obtained by applying only bioremedial-antitoxic control measure to control toxin accumulation in predators. This indicates that spatial isolation has no significant impact on the predator population since predators are not affected by diseases.

iii. Control rate by applying both spatial isolation and bioremedial-antitoxic strategies to the susceptible prey population

Both application of spatial isolation u_1 and bioremedial-antitoxic u_2 are used to optimize the objective function J.

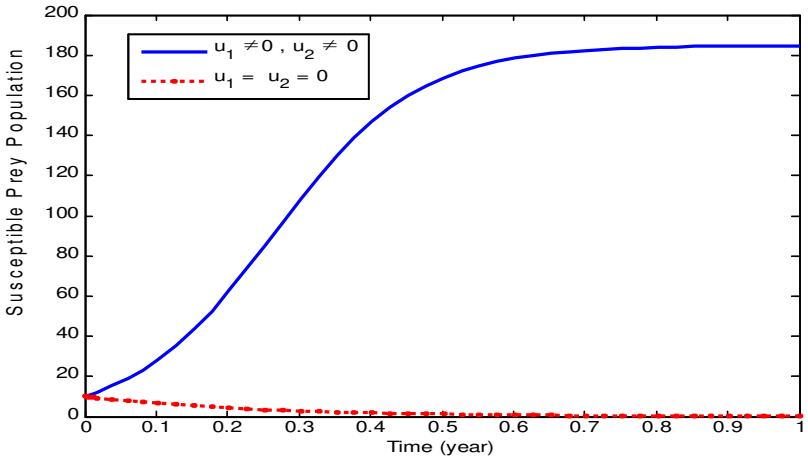

Figure 12: Effect of spatial isolation and bioremedial-antitoxic strategies on susceptible prey.

Figure 12 shows the difference before and after the implementation of two control

strategies spatial isolation and bioremedial-antitoxic on susceptible prey. Before the application of control strategies, the susceptible prey population reached extinction, as indicated by the red dotted curve. When the control strategies were simultaneously implemented, the susceptible prey population increased toward the carrying capacity by the end of the control period as shown by the blue curve. Nevertheless, Figures 4 and 8, where only one control strategy was implemented, showed differences compared to Figure 12. This indicate that both spatial isolation and bioremedial-antitoxic strategies play a significant role in controlling toxicants and diseases in susceptible prey population.

iv. Control rate by applying both spatial isolation and bioremedial-antitoxic strategies to the infected prey population.

Both application of spatial isolation u_1 and bioremedial-antitoxic u_2 are used to optimize the objective function J.

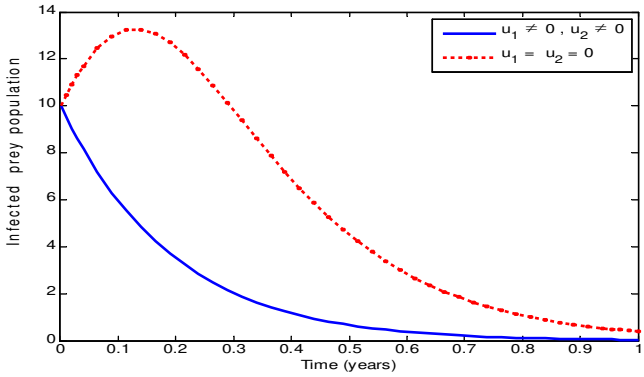

Figure 13: Effect of spatial isolation and bioremedial-antitoxic strategies on the infected prey.

Prior to control measures were applied, the infected prey population initially increased rapidly and later began to decline due to recovery (λ) deaths rate due to diseases (e) predation (N_2) and toxicants mortality rate (γ) as shown by red dotted curve. When both spatial isolation and bioremedial-antitoxic control strategies were simultaneously applied, the population directly decreased to zero as the time of control period progressed to optimal as shown by blue curve. However, Figures 5 and Figure 9 are the results when one control was applied, that differ from Figure 13 , this means that both spatial isolation and bioremedial-antitoxic strategies have a significant impact on controlling toxicants and diseases in infected prey population.

Discussion

The findings of this study reveal significant awareness into the interplay between diseases, toxicants, and population stability within prey–predator ecosystems. The proposed deterministic model, which incorporates both disease transmission among prey and toxicant accumulation in the environment, demonstrates how these challenges jointly influence species persistence. The simulations show that, in the absence of intervention, both susceptible and infected prey populations decline drastically over time, eventually leading to predator extinction due to food scarcity. This aligns with previous eco-epidemiological studies (e.g., Sinha et al., 2009; Khan and Samanta, 2020), which found that the dual threats of pollution and disease can destabilize ecosystems and accelerate species collapse.

The discussion section was based on; Disease-Prey-Predator Interactions, Influence of Toxicants, Effectiveness of individual control strategies, Collaborative effects of combined control measures, Ecological and Theoretical Implications, Comparison with previous studies, and Practical Significance subsetions.

Disease-Prey-Predator Interactions

The simulation of disease transmission among prey (Figure 1) indicates that increased infection rates result in a marked decline of the susceptible prey class, while infected prey initially rise before gradually diminishing due to mortality and recovery. This dynamic reflects a self-limiting epidemic pattern in a closed prey population. When predators are included (Figure 2), the indirect effect of disease transmission becomes evident: a reduction in susceptible prey leads to food shortage, reducing predator growth and potentially leading to extinction. These findings are consistent with Mukhopadhyay and Bhattacharyya (2009), who emphasized that host-specific diseases can critically reduce prey biomass and undermine predator survival.

Influence of Toxicants

The introduction of toxicants (Figure 3) significantly alters the system's equilibrium. Toxicants negatively affect all trophic levels, increasing mortality and reducing reproduction in both prey and predators. The model confirms that higher toxicant concentrations correspond to decreased population densities, supporting the observations of Lawaniya (2018) and Goswami et al. (2020) on the ecological consequences of pesticide contamination. This finding underscores that environmental pollution acts jointly with disease to amplify extinction risks.

Effectiveness of Individual Control Strategies

When the spatial isolation control strategy was applied alone (Figures 4 and 5), the disease transmission among prey declined substantially. The susceptible prey population increased toward its carrying capacity, while infected prey rapidly decreased to zero, suggesting that spatial separation limits contact transmission. These results agree with previous models on habitat segregation as a disease-control mechanism (Sahoo 2016).

Similarly, implementing the bioremedial-antitoxic strategy alone (Figures 6–9) effectively reduced toxicant levels and stabilized predator populations by improving environmental quality. The toxicant concentration decreased gradually to zero (Figure 7), and prey populations recovered, demonstrating that remediation efforts can reverse toxicant-induced declines. These outcomes concur with empirical findings by Goswami et al. (2020), who reported improved wildlife survival following pollution mitigation.

Collaborative effects of Combined Control Measures

The joint application of both spatial isolation and bioremedial-antitoxic controls (Figures 10–13) produced the most favorable outcomes. The susceptible prey population rebounded toward the carrying capacity, infected prey were eliminated, and predator populations stabilized. This synergy indicates that addressing both biological (disease) and chemical (toxicant) stressors simultaneously yields optimal ecological recovery. While spatial isolation alone had limited effect on toxicant concentrations, its combination with bioremediation enhanced prey health and reduced infection prevalence, illustrating a complementary relationship between the two strategies.

Ecological and Theoretical Implications

From a theoretical perspective, the model confirms boundedness and biological feasibility of solutions, implying realistic population dynamics under varying control intensities. The use of Pontryagin's Maximum Principle established the existence of optimal time-dependent controls that minimize disease and toxicant burdens while balancing associated costs. Ecologically, these findings highlight the need for integrated management practices that combine pollution control and disease mitigation to ensure long-term species coexistence. The study provides quantitative evidence supporting the ecological principle that multi-threat systems require multi-component interventions.

Comparison with Previous studies

Unlike previous works that addressed diseases or pollutants independently (e.g., Sinha et al. 2009, Zhou et al. 2018), this study simultaneously incorporated both threats and explored their optimal control. The results corroborate Khan and Samanta (2020) but extend their findings by demonstrating that the coexistence equilibrium can be restored through combined interventions. Moreover, the observed predator recovery under bioremedial-antitoxic measures supports Sagamiko et al. (2015), who found that management interventions can stabilize predator–prey interactions in threatened ecosystems.

Practical Significance

The study's outcomes have practical implications for wildlife management and conservation policy. Spatial isolation can be interpreted as habitat zoning or quarantine measures, while bioremedial-antitoxic strategies correspond to ecosystem cleanup and pollutant regulation. When implemented concurrently, these strategies can mitigate the dual effects of disease and pollution, ensuring the sustainability of both prey and predator species. Such integrative approaches are particularly relevant in ecosystems where anthropogenic activities and disease outbreaks coincide, such as national parks and conservation areas across Africa.

Conclusions

Maintaining the balance and coexistence of species in ecosystems is essential for resource management and predicting long-term survival. Prey-predator systems often show periodic dynamics, and this study examines how toxicants and diseases influence these interactions. A deterministic mathematical model was developed to analyze disease transmission in prey and the spread of toxicants affecting both prey and predators, incorporating optimal control strategies. The model assumes a Holling Type I functional response, where predator consumption increases linearly with prey populations. The study included numerical simulations, which confirmed the theoretical predictions. It established that the model remains biologically feasible, solutions are bounded and positive, the stability of equilibrium points was assessed using eigenvalue analysis (Jacobian matrix) for local stability and Lyapunov functions for global stability. Pontryagin's Maximum Principle (PMP) was used to evaluate optimal strategies for minimizing disease and toxicant effects. Control strategies were tested individually and in combination. The results showed that using both spatial isolation and bioremedial-antitoxic measures together provided the most effective threat reduction.

Recommendation

The simultaneous use of spatial isolation and Bioremedial-Antitoxic control strategies can reduce risk of prey-predator species from extinction if properly applied. Future research should explore how different Holling functional responses affect control strategies in prey-predator models impacted by toxicants and diseases on both prey and predator population.

Acknowledgements

The authors gratefully acknowledge each other's important contributions to the conception, development, and completion of this work.

References

Brauer F and Castillo-Chavez C 2001 *Mathematical models in population Biology and Epidemiology,* Springer.

Brauer F and Castillo-Chavez C 2012 *Mathematical models in populationBiology and Epidemiology(2nd ed),* Springer.

Goswami R, Dutta D and Ghosh T 2020 Pesticide Poisoning of Wildlife in Kaziranga National Park, India. *Environ. Sci. Pollut. Res*. 27(16): 2018-2029.

Hugo A and Simanjilo E 2019 Analysis of an Eco-Epidemiological Model under Optimal Control Measures for Infected Prey, Application Applied Mathematics: *An Int. Journal (AAM).*14(1):8. https://digitalcommons.pvamu.edu/aam/vol14/iss1/8

HugoA, Massawe ES and Oluwole DM 2012 An Eco-Epidemiological Mathematical Model withTreatment and Disease Infection in both Prey and Predator population, *J. Ecol. Nat. Environ.* 4(10): 266-279.

Khan N and Samanta GP 2020 Modeling the combined effects of toxicants and infectious diseases on predator-prey systems. *J. Math. Biol.* 81(2):451-474. DOI: 10.1007/s00285-019-01413-6

Kumara HN 2020 Elephant Endotheliotropic Herpesvirus: Emerging Infectious Threat in Elephant Conservation. *J. Wildl. Dis.* 56(3), 621-629.

Lawaniya P 2018 *A Study of Effect of Pollution on the Dynamics of Predator-Prey Interactions.* Ph D thesis. Deemed University, India.

Lenhart S and Workman J 2007 Optimal Control Applied to Biological Models. London, Chapman and Hall/CRC.

Mapunda A, Mureithi E, Shaban N and Sagamiko T 2018 Effects of Over-Harvesting and Drought on a Predator-Prey System with Optimal Control. *Open J. Ecol.* 8: 459-482. https://doi.org/ 10 .4236/oje.2018.88028

Massawe LN, Massawe ES and Makinde OD (2015). Modelling Infectiology and Optimal Control of Dengue Epidemic. *Appl. Comput. Math.* 3:181–191.

Mateo R 2009 Pesticide Poisoning in Spanish National Parks. *J. Wildl. Dis.*45(3), 584-596.

Miller MA 2017 Tuberculosis in Wild Elephants: Emerging Challenges in South Africa. *Vet. J.* 223: 48-54.

Miller MA 2017 Tuberculosis in Wild Elephants: Emerging Challenges in South Africa. *Vet. J.* 223: 48-54.

Ministry of Natural Resources and Tourism (MNRT) 2013 The 2013/14 Budget speech. www. parliament. go.tz/index. php/budget/.../minister retrieved on 15th May , 2013.

Mukhopadhyay B and Bhattacharyya R 2009 Role of predator switching in an eco epidemiological model with disease in the prey, *Ecol. Model.* 220: 931–939, ELSEVIER.

Nguema L 2016 "Cyanide Poisoning in Hwange National Park: A Massacre of Elephants." *J. Wildl. Conserv.* 48(2): 34-41.

Numfor E, HRilker FM and Lenhart S 2017 Optimal Culling and Biocontrol in a Predator–Prey Model. *Bull. Math. Biol.* 79(1): 88–116. https:// doi.org/ 10.1007/ s11538-016-0228-3

Ogada DL2014 The Poisoning of Africa's Wildlife. *Conserv. Biol*. 28(2): 377-388.

Ogada DL, Keesing F and Virani MZ 2015 Mass Poisoning of African Wildlife by Carbofuran. *J. Wildl. Manage.* 79(1): 25-32.

Okosun K, Makinde OD and Takaidza I (2013). Impact of optimal control on the treatment of HIV / AIDS and screening of unaware infectives. *Appl. Math. Model.* 37(6): 3802–3820.

Pada Das K, Roy S and Chattopadhyay J 2009 Effect of disease-selective predation on prey infected by contact and external sources. *Biosytems* 95: 188-199.

Riley SP, Hadidian J and Manski DA 2017 Rodenti cide Poisoning in Wildlife: Implications for Conservation. *Wildl. Res*. 44(1): 23-30.

Sagamiko TD, Shaban N, Nahonyo CLand

Makinde OD 2015 Optimal Control of a Threatened Wildebeest-Lion Prey-Predator System in the Serengeti Ecosystem. *Open J. Ecol*. 5: 110-119. https://doi.org/10.4236/oje.2015.54010

Sagamiko TD, Kozlov V and Wennergren U 2021 Predator survival analysis of a Prey-Predator system with prey species pool. *journalhomepage: www.elsevier.com /locate /sciaf.*

Sahoo B 2016 Disease control through provision of alternative food to predator: a model based study. *Int. J. Dynam. Control* 4(2): 239–253. https://doi.org/10.1007/s40435-014-0099-0

Sinha,S .,Misra.,O.P and Dhar.J 2009 Modelling a predator–prey system with infected prey in polluted environment; *Appl. Math. Model.* 34:1861–1872.

Turner WC 2020 Anthrax Outbreaks in African Herbivores: Disease Ecology and Prevention. *Ecol. Applicat.* 30(5): e02121.

Wafula MM 2008 Anthrax in Queen Elizabeth National Park, Uganda: The Role of Hippopotamuses. *Afr. J. Ecol.* 46(4), 384-391.

Xia X 2014 ”Canine Distemper Virus in Giant Pandas: A Case Study in Shaanxi, China.” *J. Zoo and Wildl. Med*. 45(2): 233-239.

Zhou Y, Zhang X and Wang H 2018 Impact of toxicants and infectious diseases on predator-prey dynamics: A Holling type-III functional response. *Ecol. Complex*. 34: 45-56. DOI: 10.1016/j.ecocom.2017.12.004